ELSEVIER

Biochimica et Biophysica Acta 1458 (2000) 188–198

BIOCHIMICA ET BIOPHYSICA ACTA
BBA

www.elsevier.com/locate/bba

Review

Mechanism of proton translocation by cytochrome *c* oxidase: a new four-stroke histidine cycle[1]

Mårten Wikström *

Helsinki Bioenergetics Group, Department of Medical Chemistry, Institute of Biomedical Sciences and Biocentrum Helsinki, P.O. Box 8, 00014 University of Helsinki, Helsinki, Finland

Received 1 November 1999; accepted 1 December 1999

Keywords: Heme-copper oxidase; Proton transfer; Energy transduction

1. Introduction

The research on the proton translocation mechanism by the haem–copper oxidases has been controversial ever since the report [1] that cytochrome *c* oxidase is a proton pump was disputed for 8 years [2–5]. Recently, Michel [6] has strongly criticised the conclusions made from titrations of oxidase reaction intermediates with phosphorylation potential in isolated mitochondria [7], and proposed a proton pump mechanism that, albeit more detailed, is related to a scheme suggested earlier by Artzatbanov et al. [8]. Our recent experimental observations, indicating the existence of a metastable 'energy-rich' form of the enzyme's binuclear haem a_3–Cu_B centre [9], are inconsistent with Michel's mechanism, and appear to break the paradigm that all proton translocation takes place *simultaneously* with the oxidative phase of the catalytic cycle where the reduced enzyme is oxidised by O_2. This paradigm was the simplest interpretation of the equilibrium titrations, which indicated that all proton translocation is linked thermodynamically to the oxidative phase [7].

Here I will briefly outline the principles of a new proton translocation mechanism of the haem–copper oxidases that has the virtue of being consistent both with our recent findings [9], as well as with the earlier observations [7]. A key feature of this mechanism is that a histidine ligand of Cu_B is intimately involved in proton translocation, as proposed earlier [10]. For comprehensive reviews of the structure and function of haem–copper oxidases, see Ferguson-Miller et al. and Gennis et al. (this issue).

2. Basic assumptions and mechanism

The following key postulates will be referred to by their respective Roman numerals.

(I) The histidine

One of the histidine ligands of Cu_B (probably His-291; Fig. 1) becomes weakly bound in the reduced binuclear Fe_{a3}–Cu_B site [18,19], and dissociates from the metal when the site reacts with CO [19]. The transient binding of O_2 to Cu_B, before binding to Fe_{a3} [20,21], may do the same by lowering the barrier

Abbreviations: Cu_A, copper ion pair in subunit II donating electrons to Fe_a; Cu_B, copper ion of binuclear oxygen binding site; E_m, midpoint or standard redox potential; eT, electron transfer; Fe_a, low-spin haem; Fe_{a3}, oxygen-binding haem; FR, fully reduced enzyme ($4e^-$); MV, mixed valence enzyme ($2e^-$ in the binuclear site); N-side, negatively charged side of the membrane; P-side, positively charged side of the membrane; q, electrical charge equivalent; RT, room temperature

* Fax: +358-9191-8296;
E-mail: marten.wikstrom@helsinki.fi

[1] Amino acid residues are numbered according to the subunit I structure of cytochrome aa_3 from bovine heart mitochondria.

PII: S0005-2728(00)00068-2

for histidine dissociation. This triggers the proton-pumping events in which the dissociated histidine is the key residue [10]. The histidine can attain three conformations: (1) bound to Cu_B; (2) dissociated input state where it can accept a proton from Glu-242; and (3) dissociated output state where it can release a proton (Fig. 1). In the two latter states, it can be either protonated ($ImHH^+$) or deprotonated (ImH). There is a barrier for return of the histidine to bind Cu_B so that the dissociated histidine has a discrete life time. This may explain why it appears to be bound to Cu_B in the crystal structure of the reduced, CO-coordinated enzyme [12].

(II) The glutamic acid and the D-channel

Glu-242 is essential for functioning of the proton pump [22]. It can attain a protonic input state where it is in contact with water molecules leading to the D-channel, or an output state where it delivers a proton either to the dissociated histidine (input state) or, when the histidine is in its output position, to the binuclear site, in both cases via two to three water molecules (Fig. 1; [14,16]).

(III) The hydrophilic cluster

The ring-D propionate of haem a_3 is connected protonically to a hydrophilic cluster of amino acid residues, relatively static water molecules, and haem propionate groups (Fig. 1; [12,13]), which collectively share a net negative charge in the ground state of the enzyme (A^- in Fig. 2A,B). However, the cluster can store one proton, the release of which to the P-side is associated with a high barrier. The 'collective' pK_a of the cluster rises when the binuclear site has excess negative charge, and perhaps also when Fe_a is reduced [23]. However, the pK_a of the cluster is always higher than the pK_a of the protonated histidine ($ImHH^+$) in its output position.

(IV) Charge separation

In the input state of the dissociated histidine, the pK_a of the imidazolium cation ($ImHH^+$) is raised by a π-cation interaction with Trp-236 at van der Waal's distance [24], and is higher than the pK_a of Glu-242. Glu-242 in its output state thus donates a proton to the imidazole to form a carboxylate-$ImHH^+$ charge pair. eT to the binuclear site increases its negative charge, which may force the charge pair apart in two ways. First, by repulsion of the carboxylate charge forcing the Glu-242 side chain to an input position where it contacts the D-channel and accepts a proton. Secondly, by attracting the $ImHH^+$, which swings out to its output position in contact with the D-ring propionate of haem a_3. Here the interaction with Trp-236 is diminished, and the pK_a decreases below that of the hydrophilic cluster. The output conformation of $ImHH^+$ allows rearrangement of the water molecules to form a proton-conducting path from Glu-242 (output) to the binuclear site. This rearrangement requires that the protonated Glu-242 is in its output conformer [16].

It is noteworthy, however, that isomerisation of the Glu-242 side chain may not always be required. This is due to an 'output' conformer than can bridge between the water molecules on each side of the residue [16]. Hence, the output protonated state may be reformed very fast by protonating the bridging conformer from the D-channel. On the other hand, if the deprotonated side chain isomerises to its input conformer, it must reisomerise after protonation to return to the output state [16]. These subtle dynamics of the Glu-242 side chain can determine the order of events during the H^+ translocation process.

(V) Proton translocation

Case A: if the cluster is unprotonated it receives a

→

Fig. 1. Proton transfer in cytochrome *c* oxidase (adapted from [11]). The view of part of the subunit I structure is in the plane of the membrane. Key residues in the D- and K-channels, and in the exit channel (hydrophilic cluster) are shown. Water molecules seen in the crystallographic models [12,13] and/or predicted by calculations [14,15] are shown as red circles. The D ring of haem a_3 is indicated, as is the hydroxyethyl group of the haem's long side chain. A hydrophobic cavity links the D-channel to Glu-242 in an input position via three water molecules [14]. A switch of the side chain (arrow) puts Glu-242 in contact with a chain of two to three water molecules [14,16]. The latter can constitute a proton transfer path to His-291 when dissociated from Cu_B. His-291 is depicted in three positions-bound to Cu_B, dissociated input position where a proton can be accepted from Glu-242, and dissociated output position in contact with the D-ring propionate of Fe_{a3} to which a proton may be delivered (arrow). The propionate brings the proton to the hydrophilic cluster above the haems, which constitutes the exit channel of the proton pump [17]. The K-channel can deliver protons from the N-side to the hydroxyethyl group and possibly to the hydroxo ligand of Cu_B. The covalent link between Tyr-244 and His-240 [12,13] is not drawn. The picture is based on the crystal structure of the mitochondrial enzyme [12].

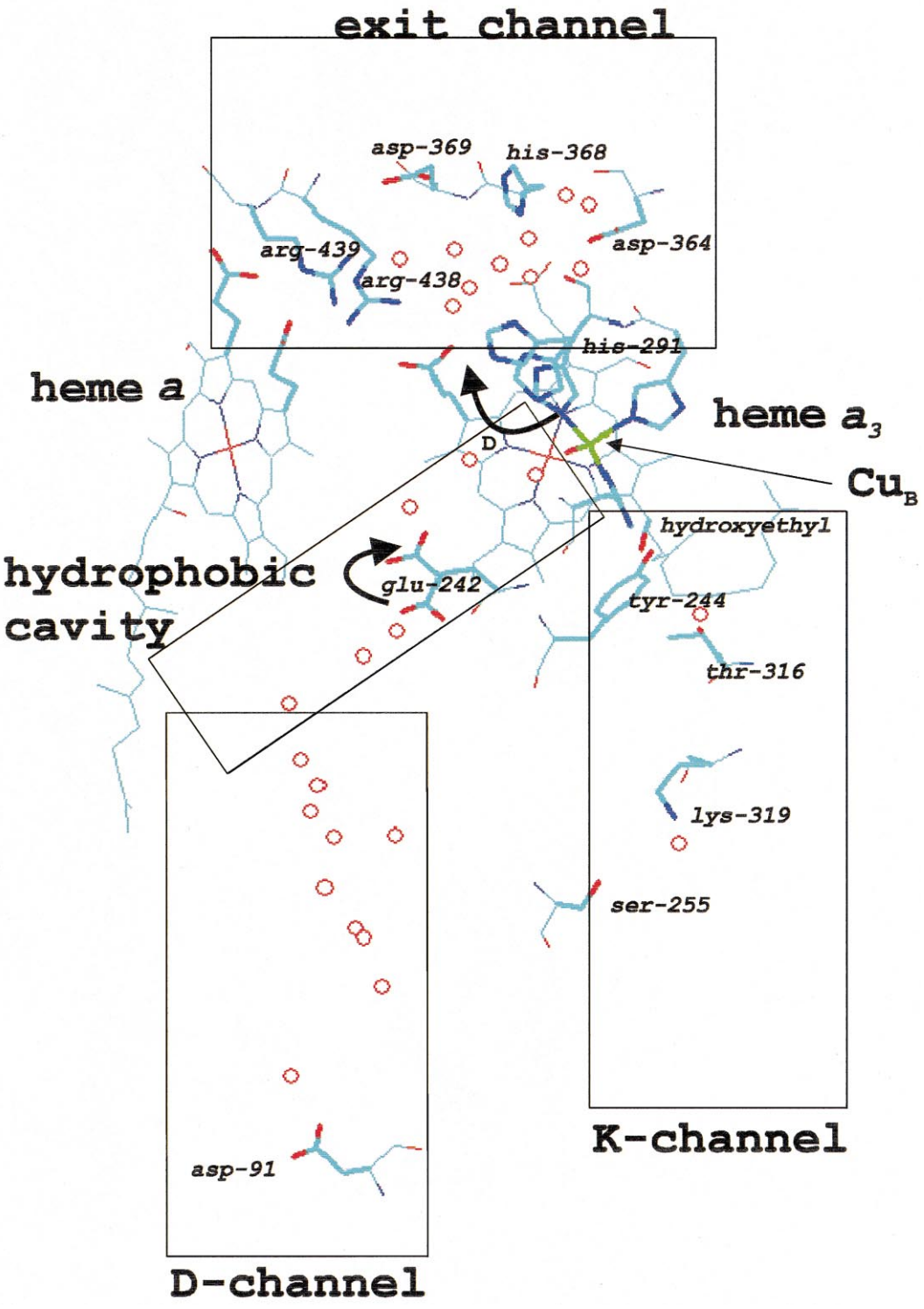
exit channel
asp-369
his-368
asp-364
arg-439
arg-438
his-291
heme a
heme a3
CuB
D
hydrophobic cavity
glu-242
hydroxyethyl
tyr-244
thr-316
lys-319
ser-255
K-channel
asp-91
D-channel

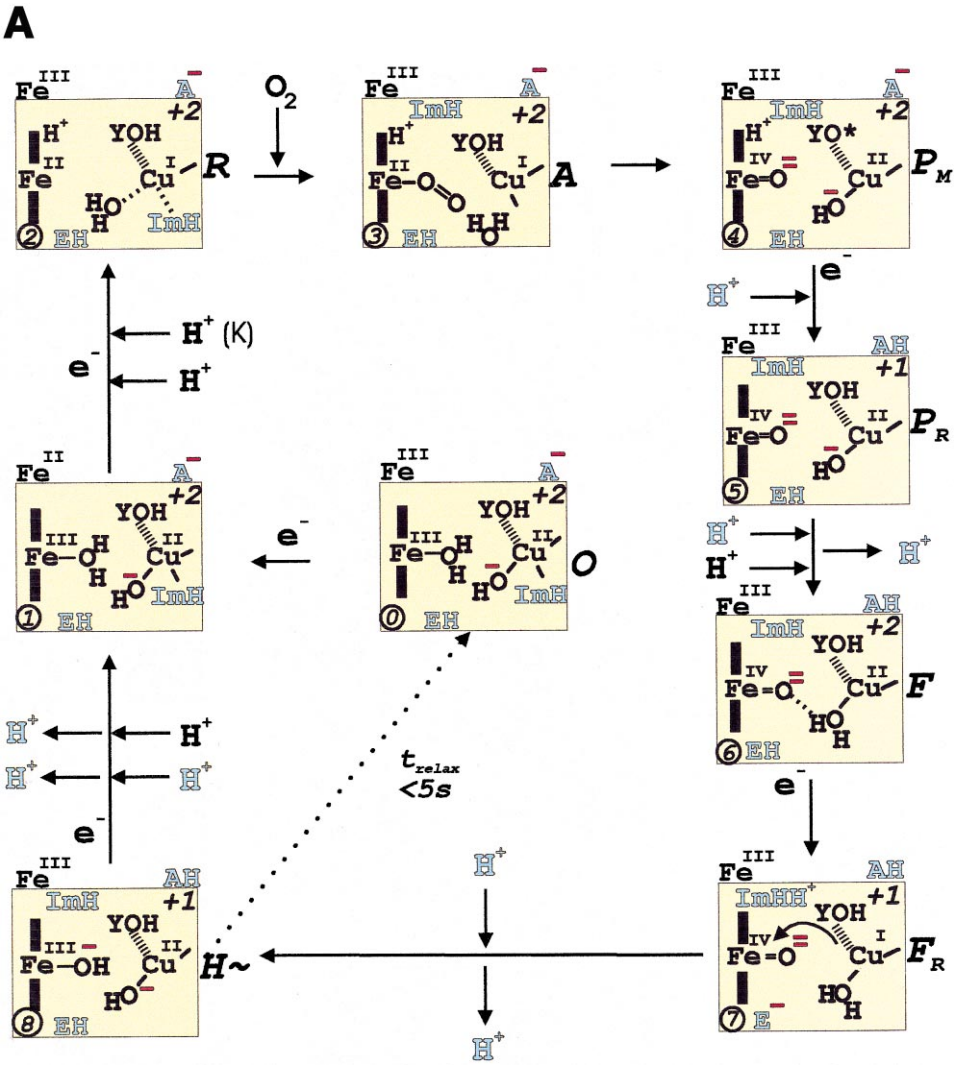

Fig. 2. Proposed reaction cycle of cytochrome *c* oxidase. (A) Cycle initiated from the mixed valence (2-electron-reduced) enzyme. (B) cycle initiated from the fully reduced ($4e^-$) enzyme. The binuclear haem–copper domain is depicted inside the box, which also includes the residue Glu-242 (EH). The circled number in the lower left corner is the state number. The number in the upper right corner is the formal electrical charge of the domain within the box, which should be used only for comparison between states. Only the 6th axial ligand of Fe_{a3} is shown. Some states are named with a letter code on the right-hand side outside the box. P stands for a state with the characteristic 607-nm optical absorption band, F for a state with the characteristic 580-nm band (see Addendum). H stands for a state with a hydroxo ligand on ferric Fe_{a3} (see [32]). H∼ is an occluded 'high-energy' state with potential for proton translocation (see text). O is the oxidised site, R the reduced site and A is the dioxygen adduct. The Fe above the box depicts the redox state of Fe_a. Note that in Fig. 2B Fe_a has been re-reduced by Cu_A in state F, and that a total of four electrons are required to reform the R state. The A above the box is a collective denotation of the hydrophilic cluster of residues on the P-side of the haem groups (see text). Cu_B has three histidine ligands, and one OH^- ligand in state O [33]. One histidine (His-240, not shown) is covalently bonded to Tyr-244 [12,13,34]. This is indicated by a crossbar from Cu to YOH, where YOH is the tyrosine, which is suggested to form the neutral radical Y* in some states [13,35,36]. A second histidine is only depicted as a bond from Cu, and a third as the neutral imidazole (ImH). The latter can dissociate from the copper and be protonated to the imidazolium cation ($ImHH^+$). When dissociated, the imidazole can attain protonic input and output states (see text). Proton uptake from the N-side is shown from the inside of the scheme and proton release to the P-side on the outside. Protons coloured black are destined for consumption in the O_2 reduction chemistry. Blue protons are pumped. All protons taken up from the N-side, except when labelled (K), are taken up via the D-channel. Note that for reasonable brevity, some intermediate reaction steps have been omitted.

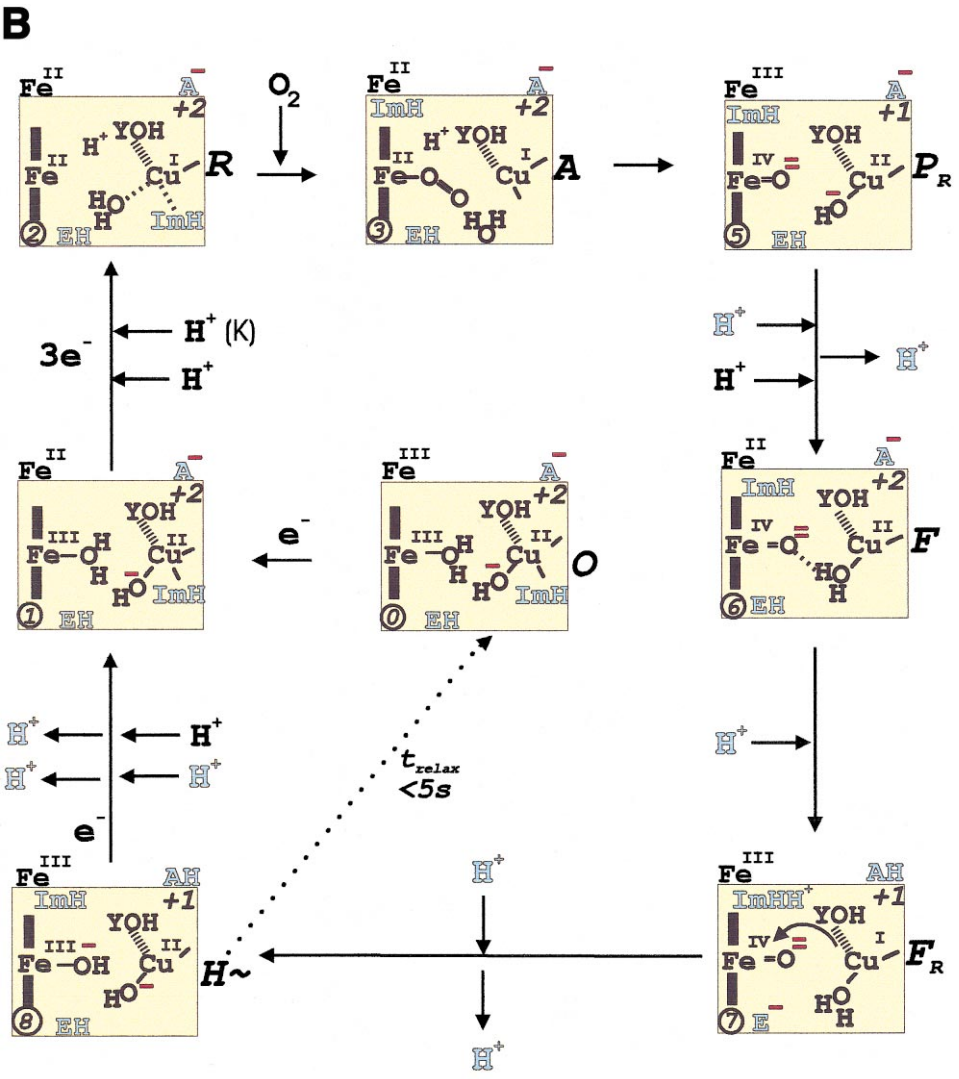

Fig. 2 (*continued*)

proton from $ImHH^+$, and the neutral imidazole returns to its input state. Note, that this may occur before or after Glu-242 has reached its protonated output conformer. Only if Glu-242 is quickly reprotonated (see above), will there be time for a proton path to be formed to the binuclear site. *Case B*: If the cluster is protonated, it cannot accept the proton from $ImHH^+$, which cannot return to its input conformer until the excess negative charge in the binuclear site has been neutralised. Hence, the side chain of Glu-242 (input) has time to isomerise to its output conformer, which helps the water molecules to rearrange to provide a proton transfer path directly into the binuclear centre. This is not possible unless the histidine is in its output position. Proton transfer from Glu-242 now neutralises the binuclear site. This decreases the pK_a of both $ImHH^+$ (output) and the cluster (AH), but the pK_a of the latter remains higher. The cluster donates its proton to the P-side of the membrane, and is reprotonated by $ImHH^+$. The Glu-242 anion returns and is reprotonated from the D-channel. The cluster can retain the proton for a long time, relative to the turnover rate, due to the high barrier for its release.

(VI) K-channel

This proton-conduction path (Fig. 1) connects to the binuclear site when the D-channel is closed, but proton transfer may be intrinsically slow as com-

pared to that through the D-channel. Proton transfer via the K-channel occurs specifically when the oxidised ferric/cupric binuclear site (state O) is reduced to the ferrous/cuprous state R (see [25]), a reaction that is associated with net uptake of two protons [26].

(VII) The high-potential Cu_B

After dissociation of the histidine ligand from Cu_B, converting it to a trigonal structure, the E_m of the cupric/cuprous redox pair is raised by >0.5 V due to the large difference in binding energy for the fourth ligand in these two oxidation states (see e.g. [27]). A priori, this increases the electron affinity of the trigonal Cu_B above that of the oxoferryl haem a_3 so that Cu_B will be reduced by the incoming electron. However, neutralisation of the hydrophilic cluster, *together* with $ImHH^+$ in its output state (but not each alone), elevates the E_m of the oxoferryl iron above that of Cu_B, which is necessary to allow eT from the high-potential Cu_B to the oxoferryl haem iron.

(VIII) Fully reduced and mixed valence enzyme

The reactions of fully reduced (FR) and mixed valence (MV) enzyme with O_2 are different. While both these states first form the O_2 adduct, compound A, in about 8 μs (see [28]), the FR enzyme continues by fast electron transfer from Fe_a to the binuclear site [21,29], which forms the intermediate P_R [30], followed by other intermediates, and ultimately the fully oxidised enzyme. In contrast, with no electron available at Fe_a, the MV enzyme relaxes in ca. 200 μs to intermediate P_M [28], which appears relatively stable.

3. Reaction cycle

When the reduced site (R) reacts with O_2 the oxygen adduct, compound A, is formed (see [28]) with release of the histidine ligand of Cu_B (I). One Cu_B ligand is 'missing' in this state (Fig. 2), and this might be a Cl^- ion, as recently observed [19]. With no electron available at Fe_a, compound A relaxes in 200 μs to P_M (Fig. 2A, state 4). A hydroxoperoxide state is an unstable intermediate in this O–O bond splitting reaction [31]. The 'extra' proton shown in states R, A and P_M is bound to the hydroxyethyl group of the hydroxyethyl-farnesyl side chain of haem a_3, in close vicinity to the oxygen atom of Tyr-244. This hydroxyethyl group is basic when the haem iron is in the ferrous or oxoferryl state, and the bound proton is essential for lowering the barrier for O–O bond scission [31].

Michel [6] proposed that the P_M state relaxes spontaneously to an F-like state with the pumping of one proton, but this is very unlikely because of the known stability of P_M. Indeed, the formal charge of the binuclear site is +2, as it is in the relaxed state O (Fig. 2A). The potential energy of the P_M state lies in its three highly oxidising redox centres that were generated by the O–O bond splitting reaction [31], and becomes available only upon electron transfer.

Electron transfer into P_M (Fig. 2A) triggers the charge separation event (IV), and proton translocation occurs (V, case A). The proton in $ImHH^+$ is deposited in the hydrophilic cluster, and the imidazole side chain returns to its input state before reprotonation of Glu-242 and formation of a proton conduction path to the binuclear site has time to occur. It is possible that the reduction of Fe_a in P_M already induces the charge separation, which might account for the fast return of the imidazole. This is the first proton-pumping step, although without net proton release on the P-side. Reduction of the high-potential tyrosine radical attracts the nearby proton at the hydroxyethyl group, neutralising the tyrosine.

In contrast, if an electron is available from the beginning at Fe_a (FR enzyme, Fig. 2B), the P_M state is by-passed in a fast 30 μs electron transfer step that forms P_R directly [28–30]. The first proton-translocating step fails to occur, and the hydrophilic cluster retains its delocalised negative charge (Fig. 2B, state 5). One reason for this bypass might be that, in the fully reduced enzyme, the 30 μs eT from Fe_a to the binuclear site after binding of O_2 is too fast to allow for proton translocation. Interestingly, the by-pass of an early proton-pumping step when starting the O_2 reaction from the fully reduced enzyme was already suspected earlier [28], but was later neglected.

The P_R state is metastable [30] due to excessive negative charge in the binuclear site (+1). If the cluster is already neutralised (Fig. 2A, state 5), charge separation is followed by fast reprotonation of Glu-242 from the N-side, and transfer of the proton to the binuclear site to form an aquo ligand on Cu_B (V, case B). This causes release of the proton in the

cluster to the P-side, but it is immediately reprotonated by the $ImHH^+$ cation, and the cluster remains protonated (III; Fig. 2A, state 6).

If the cluster is deprotonated in P_R (Fig. 2B), charge separation (IV) occurs followed by protonation of the cluster (V; case A). Reprotonation of Glu-242 is fast and proton transfer into the binuclear site has time to occur, converting the hydroxo ligand of Cu_B into water. This again pushes the proton in the cluster across its barrier into the P-side of the membrane by electrostatic repulsion, but this time the cluster cannot be reprotonated. Such electrostatic repulsion by uptake of the proton required in the O_2 reduction chemistry has been suggested earlier as one of the basic principles of driving proton translocation [8,10,37], and was also adopted in Michel's mechanism [6]. Finally, Glu-242 is reprotonated and a 'relaxed' F state is formed with the cluster deprotonated (Fig. 2B, state 6).

Electron transfer into the F state reduces Cu_B, the E_m of which initially exceeds that of the oxoferryl haem (VII). If the cluster is unprotonated (Fig. 2B), it must first receive a proton from $ImHH^+$ after charge separation, as before (not shown), with uptake of a proton from the N-side into Glu-242. The F_R state is metastable (charge +1) but eT from Cu_B to Fe_{a3} is still thermodynamically unfavourable (VII). Charge separation (shown in state 7, Fig. 2B) with formation of $ImHH^+$ compensates for the deficient positive charge in the binuclear site, and now raises the E_m of the oxoferryl haem above that of Cu_B. eT takes place within the binuclear site coupled to translocation of one proton.

In the case where the cluster is already protonated in F (Fig. 2A, state 6), electron transfer into Cu_B and the following charge separation (state 7) are alone sufficient to reach the transition state for eT within the site, which relaxes with translocation of one proton, as before. Note that when the F state is 'relaxed' with the cluster unprotonated (as in Fig. 2B), *two* proton-translocating events are required to achieve eT within the centre, whereas *one* such event suffices when the cluster is 'charged' (pre-protonated).

An 'occluded' metastable state is now reached ($H\sim$, Fig. 2A,B) with potential for proton translocation, but with no proton transfer path [9]. In this state, the proton in the cluster is held by electrostatic attraction to the excess negative charge in the binuclear site (+1). The $H\sim$ state was originally called $O\sim$ [9], but the new name is due to our suggestion that it contains Fe_{a3} with a hydroxo ligand, as was already considered by Rousseau [32]. $H\sim$ relaxes spontaneously to the oxidised state O with a time constant of ca. 1–2 s ([9] and unpublished data). However, if the next electron arrives *before* this relaxation, charge separation occurs (IV) followed by the uptake of two protons from the N-side and release of two protons to the P-side (V, case B), as observed [9]. A relaxed O state is reached with an electron at Fe_a (state 1; however, see below).

The precise way by which electron transfer into the $H\sim$ state causes its relaxation is not known. Two major scenarios may be considered: eT into Fe_a might suffice, or reduction of Cu_B might be required. $H\sim$ is basically a metastable state (charge +1), which in P_R, for example, was in itself sufficient to spontaneously initiate proton translocation. This difference might be related to the much slower time domain in which the $F\rightarrow H\sim$ transition occurs (1–3 ms), as compared to $P\rightarrow F$ (100 μs), so that the histidine ligand may have time to return to bind to Cu_B (I). Reduction of Cu_B might be required to initiate relaxation, which would be linked to uptake of *three* protons from the N-side (and release of two to the P-side), the additional one to protonate the hydroxo ligand of Cu_B (not shown). However, as drawn in Fig. 2, we presently favour the scenario where reduction of Fe_a is sufficient to trigger charge separation. Admittedly, the role – if any – of Fe_a in proton translocation remains enigmatic. The loss of the positive charge at Fe_a upon its reduction might be sufficient to favour charge separation and subsequent proton translocation *especially when the binuclear site has excessive negative charge*.

In Fig. 2A,B, the reduction of the binuclear site metals to create the R state is coupled to the uptake of two protons [26], one to make an aquo ligand at the reduced Cu_B site, and another to bind to the hydroxyethyl group of Fe_{a3}. At least the latter proton transfer step, but possibly both, will occur via the K-channel.

4. Comparison to experimental data

It is interesting that on the phenomenological lev-

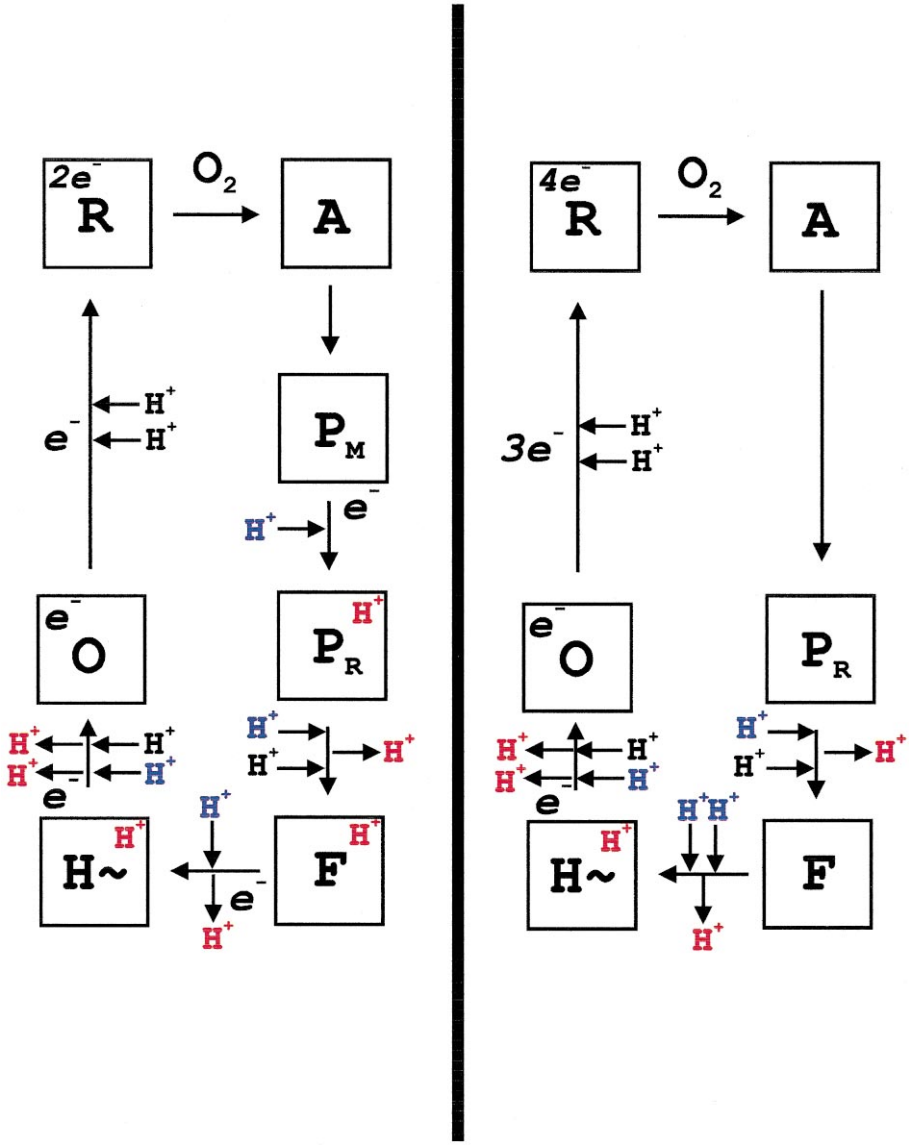

Fig. 3. Simplified schematic comparison of the catalytic cycles initiated from mixed valence (left) and fully reduced enzyme (right). The states of the binuclear site are named as in Fig. 2. Black protons are consumed in the oxygen reduction chemistry. Blue protons are taken up from the N-side to be pumped across the dielectric, to be released as red protons on the P-side. A red proton inside the state box denotes protonation of the hydrophilic cluster above the haem groups, i.e. it has essentially crossed the dielectric barrier (see the text).

el, at which no mechanism is specified (Fig. 3), this model agrees with the equilibrium data from 1989 [7] as well as with the recent dynamic results [9]. There is a particularly striking agreement with the ingenious steady-state experiments of Vygodina et al. [39], which show translocation of four protons in the 'peroxidase half reaction', where H_2O_2 converts the O state into P_M, which is reduced back to O by a high-potential electron source. The observed rate of turnover (0.26 s^{-1}; [38]) is consistent with relaxation of H~ to O in the cycle. The model also agrees with the electrometric data for the fully reduced enzyme reacting with O_2 [39], but it is not at first sight consistent with the charge separation measured upon electron injection into the F [40] or P_M states [41]. In both cases, the initial reduction of Fe_a leads to subsequent slower charge translocation, the amplitude of which is 4–5 times the amplitude during eT

to Fe_a. Recently, we have shown that eT between Cu_A and Fe_a takes place across 0.32 of the dielectric [9], which means that only ca. 1.3–1.6 q would be translocated in the steps $P_M \rightarrow F$ and $F \rightarrow O$, in contrast to the present model (Fig. 3, left). In these experiments, the P_M state is made by H_2O_2 or $CO+O_2$ treatment of the oxidised enzyme, and the F state is produced with excess H_2O_2. In the present model, the reaction of the O state with H_2O_2 is indeed expected to yield P_M via an unstable ferric hydroperoxy state. The reduction of the site by CO in the presence of O_2 will produce P_M in a similar fashion. The two protons released in this reaction will bind to the hydroxo ligand of Cu_B and the hydroxyethyl group of Fe_{a3}, respectively.

In these procedures, there is ample time for the dissociated histidine to cross the barrier and ligate back to Cu_B (I). The P_M state may thus be expected to relax to a state with a tetragonal, low potential Cu_B. Injection of an electron will quickly reduce the tyrosine radical, but without charge separation, and thus the first proton translocation step may be bypassed. The dynamics of the histidine dissociation from Cu_B and its rebinding may indeed be an essential feature of the proposed pump mechanism.

Injection of an electron into the F state is expected to yield translocation of either 1 (Fig. 3, left) or 2 (Fig. 3, right) charges, depending on the protonation state of the hydrophilic cluster in F. The observation of ca. 1.6 q translocated in this reaction [40], using our value for the relative dielectric depth of Fe_a (see above), could thus mean that the cluster in the F state has been protonated to ca. 50%. In the steady-state procedure of making F by reacting the O state with excess H_2O_2, P_M is formed first, but immediately reduced to F by a second peroxide molecule. Thus, a 50/50 population of F states may well form with the hydrophilic cluster protonated and deprotonated.

Equilibrium titrations of the $O \rightarrow F$ transition with phosphorylation potential in intact mitochondria [7] indicated a total of 2.8–3.0 translocated charges (q) for this step at neutral pH. Fig. 3 (left) shows that this step leads to translocation of about 3 q, including moving one proton towards the N-side from the binuclear site, and moving one electron out of Fe_a, in reasonable agreement with the data in [7]. This is because in F, one of the protons taken up from the P-side in the reverse reaction will remain bound to the hydrophilic cluster on that side. Clearly, we must assume that the O state reverses to $H\sim$ at high protonmotive force, which favours the possibility that it is eT into Fe_a and not into Cu_B that discharges this state in the forward reaction (cf. above).

At alkaline pH, the number of charges translocated in the $O \rightarrow F$ step was found to be reduced to ca. 2.2 [7]. The reason for this might simply be that at high pH one proton is pulled out via the D-channel from the binuclear site to yield an H state, which is indistinguishable from O by optical spectroscopy. Although such an event may be expected to be slow on a turnover time scale, it may well occur in an equilibrium situation. From our knowledge of the relative dielectric depth of the binuclear site [9], such deprotonation will occur across ca. 0.68 of the dielectric barrier, which when subtracted from 2.8–3.0 q, yields 2.1–2.3 q, in good agreement with the experimental result [7].

The total number of charges translocated between the F and P_M states at high protonmotive force was estimated to be 3.6–4.0 [7]. In Fig. 3 (left panel) only 3.0 q are predicted, including the electron transfer out of Fe_a. However, considering the structure of P_M (Fig. 2A, state 4), it is conceivable that the proton bound to the hydroxyethyl group is pulled out to the N-side via the K-channel at high protonmotive force (ca. 0.68 q). In addition, protonation of the hydrophilic cluster from the P-side may occur. Hence, it is easily possible that close to one additional charge equivalent is effectively translocated across the dielectric at high protonmotive force, in line with the observation in [7].

5. Epilogue

It must be emphasised that the mechanism presented here is still at a working stage, and that it will need considerable refinement and specification of the key events from new experimental information. This proposal has been driven by the desire to test a relatively directly coupled mechanism for proton translocation, i.e. one that does not in its most fundamental events require large conformational changes and that, therefore, can be more easily refuted by experiment. Though the mechanism includes

specified conformational changes, these are restricted to isomerisations of amino acid side chains and reorganisation of water molecules. However, it is perhaps even likely that further changes in conformation may be necessary, e.g. to control the water structure and proton transfer in the hydrophobic cavity surrounding Glu-242.

Acknowledgements

I am indebted to my colleagues in the Helsinki Bioenergetics Group, especially Joel Morgan and Michael Verkhovsky, for numerous discussions and criticism, and for their excellent experimental skills. I also wish to thank Gerald Babcock, Margareta Blomberg, Peter Brzezinski, Harry Gray, Gerhard Hummer, Ken Karlin, Marvin Makinen, Régis Pomès, Denis Rousseau, Per Siegbahn, and William Woodruff for several helpful suggestions and ideas.

Addendum. The optical spectral difference between the P and F structures

The optical spectra of P and F are very different in the α/β region [42], and these spectra derive primarily from the Fe_{a3} group. In the past, this made us reluctant to accept the notion that the O–O bond has been broken in both species, and particularly that both could have the same oxyferryl haem structure. As pointed out before [43], the difference spectrum of P with its sharp peak at 607 nm with high molar absorptivity is reminiscent of the properties of low spin ferrous haem A (cf. ferrous *minus* ferric Fe_a absorbing at 605 nm). Also in the Soret, there is a red shift from the ferric form, but the absorptivity is far less than for a ferrous haem [43]. In contrast, F has a broad absorption band at 580 nm with reduced intensity, while the Soret band is almost the same as for P. In fact, the spectrum of F is reminiscent of a low spin *ferric* haem A (cf. Fe_{a3}–CN complex).

Gennis [36] suggested that the P spectrum may derive from H-bonding on the distal side of Fe_{a3}. This was put more explicitly by Michel [6], who proposed that the unique P spectrum may be due to a strong H-bond between the oxo group of Fe_{a3} and the hydroxo ligand of Cu_B. This would mean, implicitly, that when the hydroxo ligand is protonated to water in the F state, this water molecule leaves the site and the loss of hydrogen bonding to the oxo group is responsible for the spectral change. In contrast, as Proshlyakov et al. [35] pointed out by comparison with myeloperoxidase data [44], an F-like spectrum may be expected when there is *stronger* H-bonding to the oxoferryl group and a P-like spectrum with *weaker* H-bonding. They also considered that the tyrosine radical in P might contribute to the difference, but this is in contrast to the observation [30] that the spectrum of P_R (without tyrosine radical) is identical to that of P_M.

Oxoferryl haems are known to have optical spectra quite similar to the corresponding ferrous low spin haems, which is why the oxoferryl structure was early considered for the P state [43]. In fact, as pointed out by Graham Palmer (personal communication), the shape and extinction of the P spectrum in the α/β-band is closely reminiscent of the spectra of the ferrous Fe_{a3} centre complexed with CO or O_2, albeit red-shifted by some 15 nm. This may not be surprising considering that the isolated ferryl oxo group has very little partial charge [45]. Hence, the haem macrocycle becomes essentially electroneutral, as it is in ferrohaem. Therefore, in P there may be only weak H-bonding to the oxo group [46]. In contrast, if the Cu_B *retains* the aquo ligand in the F state (Fig. 2), there may be stronger H-bonding to the oxo group. Electron donation to Fe_{a3} diminishes, and the haem may be more symmetrical. The former tends to increase the energy of the α-band (blue shift relative to P), and the latter would decrease the intensity of the absorption. It is concluded that the present oxoferryl structures of the P and F states can account for the observed difference in optical spectra.

References

[1] M. Wikström, Nature 273 (1977) 271–273.
[2] J. Moyle, P. Mitchell, FEBS Lett. 88 (1978) 268–272.
[3] K. Krab, M. Wikström, FEBS Lett. 91 (1978) 8–14.
[4] M. Wikström, R. Casey, FEBS Lett. 183 (1985) 293–298.
[5] P. Mitchell, R. Mitchell, A.J. Moody, I.C. West, H. Baum, J. Wrigglesworth, FEBS Lett. 188 (1985) 1–7.
[6] H. Michel, Proc. Natl. Acad. Sci. USA 95 (1998) 12819–12824.
[7] M. Wikström, Nature 338 (1989) 776–778.

[8] V.Y. Artzatbanov, A.A. Konstantinov, V.P. Skulachev, FEBS Lett. 87 (1978) 180–185.
[9] M.I. Verkhovsky, J.E. Morgan, M. Wikström, Nature 400 (1999) 480–483.
[10] J.E. Morgan, M.I. Verkhovsky, M. Wikström, J. Bioenerg. Biomembr. 26 (1994) 599–608.
[11] M. Wikström, Curr. Opin. Struct. Biol. 8 (1998) 480–488.
[12] S. Yoshikawa, K. Shinzawa-Itoh, R. Nakashima, R. Yaono, E. Yamashita, N. Inoue, M. Yao, M.J. Fei, C.P. Libeu, T. Mizushima, H. Yamaguchi, T. Tomizaki, T. Tsukihara, Science 280 (1998) 1723–1729.
[13] C. Ostermeier, A Harrenga, U. Ermler, H. Michel, Proc. Natl. Acad. Sci. USA 94 (1997) 10547–10553.
[14] S. Riistama, G. Hummer, A. Puustinen, R.B. Dyer, W.H. Woodruff, M. Wikström, FEBS Lett. 414 (1997) 275–280.
[15] I. Hofacker, K. Schulten, Proteins 30 (1998) 100–107.
[16] R. Pomès, G. Hummer, M. Wikström, Biochim. Biophys. Acta 1365 (1998) 255–260.
[17] A. Puustinen, M. Wikström, Proc. Natl. Acad. Sci. USA 96 (1999) 35–37.
[18] J.P. Osborne, N.J. Cosper, C.M.V. Stålhandske, R.A. Scott, J.O. Alben, R.B. Gennis, Biochemistry 38 (1999) 4526–4532.
[19] M. Ralle, M.L. Verkhovskaya, J.E. Morgan, M.I. Verkhovsky, M. Wikström, N.J. Blackburn, Biochemistry 38 (1999) 7185–7194.
[20] W.H. Woodruff, O. Einarsdottir, R.B. Dyer, K.A. Bagley, G. Palmer, S.J. Atherton, R.A. Goldbeck, T.D. Dawes, D.S. Kliger, Proc. Natl. Acad. Sci. USA 88 (1991) 2588–2592.
[21] M.I. Verkhovsky, J.E. Morgan, M. Wikström, Biochemistry 33 (1994) 3079–3086.
[22] M.L. Verkhovskaya, A. Garcia-Horsman, A. Puustinen, J.-L. Rigaud, J.E. Morgan, M.I. Verkhovsky, M. Wikström, Proc. Natl. Acad. Sci. USA 94 (1997) 10128–10131.
[23] A. Kannt, C.R.D. Lancaster, H. Michel, Biophys. J. 74 (1998) 708–721.
[24] J.P. Gallivan, D.A. Dougherty, Proc. Natl. Acad. Sci. USA 96 (1999) 9459–9464.
[25] P. Brzezinski, P. Ädelroth, J. Bioenerg. Biomembr. 30 (1998) 99–107.
[26] R. Mitchell, P. Mitchell, P.R. Rich, Biochim. Biophys. Acta 1101 (1992) 188–191.
[27] A.J. Di Bilio, C. Dennison, H.B. Gray, B.E. Ramirez, A.G. Sykes, J.R. Winkler, J. Am. Chem. Soc. 120 (1998) 7551–7556.
[28] G.T. Babcock, M. Wikström, Nature 356 (1992) 301–309.
[29] S. Han, Y.C. Ching, D.L. Rousseau, Proc. Natl. Acad. Sci. USA 87 (1990) 8408–8412.
[30] J.E. Morgan, M.I. Verkhovsky, M. Wikström, Biochemistry 35 (1996) 12235–12240.
[31] M.R.A. Blomberg, P.E.M. Siegbahn, G.T. Babcock, M. Wikström, J. Biol. Inorgan. Chem., in press.
[32] D.L. Rousseau, Nature 400 (1999) 412–413.
[33] Y.C. Fann, I. Ahmed, N.J. Blackburn, J.S. Boswell, M.L. Verkhovskaya, B.M. Hoffman, M. Wikström, Biochemistry 34 (1995) 10245–10255.
[34] G. Buse, T. Soulimane, M. Dewor, H.E. Meyer, M. Blüggel, Protein Sci. 8 (1999) 985–990.
[35] D.A. Proshlyakov, M.A. Pressler, G.T. Babcock, Proc. Natl. Acad. Sci. USA 95 (1998) 8020–8025.
[36] R.B. Gennis, Biochim. Biophys. Acta 1365 (1998) 241–248.
[37] P.R. Rich, Aust. J. Plant Physiol. 22 (1995) 479–486.
[38] A. Jasaitis, M.I. Verkhovsky, J.E. Morgan, M.L. Verkhovskaya, M. Wikström, Biochemistry 38 (1999) 2697–2706.
[39] T.V. Vygodina, N. Capitanio, S. Papa, A.A. Konstantinov, FEBS Lett. 412 (1997) 405–409.
[40] D. Zaslavsky, A.D. Kaulen, I.A. Smirnova, T. Vygodina, A.A. Konstantinov, FEBS Lett. 336 (1993) 389–393.
[41] S. Siletsky, A.D. Kaulen, A.A. Konstantinov, Biochemistry 38 (1999) 4853–4861.
[42] M. Wikström, J.E. Morgan, J. Biol. Chem. 267 (1992) 10266–10273.
[43] M. Wikström, K. Krab, M. Saraste, Cytochrome Oxidase: A Synthesis, Academic Press, London, 1981.
[44] W.A. Oertling, H. Hoogland, G.T. Babcock, R. Wever, Biochemistry 27 (1988) 5395–5400.
[45] D.T. Sawyer, Oxygen Chemistry, Oxford University Press, New York, 1991.
[46] D.A. Proshlyakov, T. Ogura, K. Shinzawa-Itoh, S. Yoshikawa, T. Kitagawa, Biochemistry 35 (1996) 76–82.